JCTC Journal of Chemical Theory and Computation

pubs.acs.org/JCTC Article

Performance of Screened-Exchange Functionals for Band Gaps and Lattice Constants of Crystals

Cheng Zhang, Pragya Verma, Jiaxu Wang, Yiwei Liu, Xiao He, Ying Wang,* Donald G. Truhlar,* and Zhonghua Liu*

Cite This: *J. Chem. Theory Comput.* 2023, 19, 311−323 Read Online

ACCESS | Metrics & More | Article Recommendations | Supporting Information

ABSTRACT: Kohn−Sham density functional theory is the most widely used method for electronic structure calculations of solid-state systems. The screened-exchange functionals developed following the influential work of Scuseria and co-workers in 2003−2006 have significantly improved the accuracy of the predictions of solid-state properties. This work assesses six screened-exchange density functionals for the prediction of 60 band gaps (database BG60) and 68 lattice constants (database LC68). The band gaps are calculated with both consistently calculated lattice constants and experimental lattice constants. Results for the nonlocal screened-exchange functionals are compared with those for six widely used or recently developed local functionals. The results show that all the screened-exchange functionals have smaller mean absolute errors (MAEs) than any of the local functionals. All the functionals except HLE17 overestimate (on average) the lattice constants, and M06-SX gives the best performance among the compared functionals, with a MAE of 0.051 Å. All the functionals underestimate (on average) the band gaps, and M06-SX outperforms all other functionals, with a MAE of 0.47 eV. M06-SX also has the lowest root-mean-squared error for both LC68 and BG60. For the subdatabases of BG60, M06-SX shows better performance for ionic crystals and systems with large band gaps, while HSE12s gives better results for semiconductors and systems with small band gaps. Overall, M06-SX shows the best performance for solid-state systems, followed by N12-SX and HSE12s. The best-performing local functionals are M06-L, revM06-L, and HLE17 for band gaps and M06-L and revM06-L for lattice constants. We found that M06-SX, revM06-L, and N12-SX not only are well optimized for a broad array of chemical properties but also have very good performance for the databases in this paper, making them well-suited for applications involving heterogeneous chemistry.

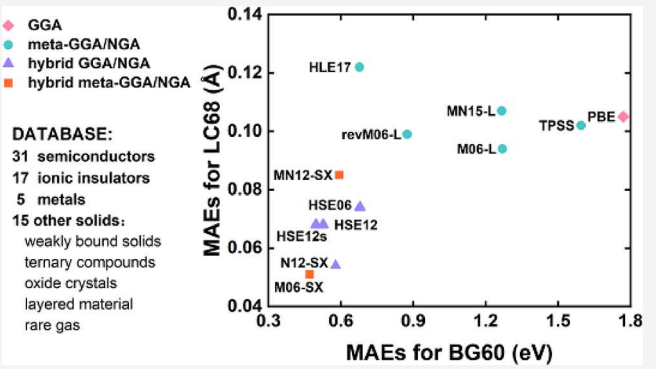

1. INTRODUCTION

Kohn−Sham density functional theory (KS-DFT) is a powerful tool in physics, chemistry, and materials.[1−4] In the present work, we are especially focused on its ability to aid material design and evaluation by predicting the lattice constants and band gaps of crystals.[5−10] The band gap is an important optical and electrical property of materials and it plays a key role in the design of semiconductor devices, batteries, and photocatalytic schemes, among others.[11−14] The lattice constant has an important effect on many other properties, including band gaps.[15,16]

Although KS-DFT is in principle exact, the accuracy in practice is limited by the necessarily approximate nature of the exchange−correlation (XC) functionals.[17,18] The original density functionals involved only the local electron spin density. Later progress involved other local properties such as density gradients (as in gradient approximations (GAs), i.e., generalized gradient approximations (GGAs)[19−21] and non-separable gradient approximations (NGAs)) and kinetic energy densities (as in meta GAs, i.e., meta-GGAs and meta-NGAs). The most popular local functional in solid-state physics is the PBE functional,[22] which is a GGA proposed in 1996. As compared to local spin density approximations (LSDAs),[23] GGAs reduce the underestimation of lattice constants and improve the accuracy of band gap predictions.[20,24−27] The meta-GGAs,[28−34] such as TPSS[32] and M06-L,[34,35] add the kinetic energy density to the components of a GGA,[36] but although they yield more accurate chemical properties they do not necessarily improve the prediction accuracy for the properties of solids.[37−39] The functionals mentioned so far are local functionals, which means that the

Received: August 10, 2022
Published: December 15, 2022

Table 1. All the Solid-State Systems Calculated in This Work[a]

semiconductors	C (227), Si (227), Ge (227), SiC (216), BP (216), BAs (216), AlP (216), AlAs (216), AlSb (216), GaN (216), GaN (186), GaP (216), GaSb (216), GaAs (216), InN (186), InP (216), InAs (216), InSb (216), MgS (216), MgSe (225), MgTe (216), BaS (225), BaSe (225), BaTe (225), ZnO (186), ZnS (216), ZnSe (216), ZnTe (216), CdS (216), CdSe (216), CdTe (216)
ionic insulators	Al_2O_3 (167), LiH (225), LiF (225), LiCl (225), NaF (225), NaCl (225), KF (225), KCl (225), MgO (225), CaF_2 (225), AgCl (225), AgBr (225), AgI (216), CuCl (216), CuBr (216), CuI (216), RbBr (225)
metals	Li (229), Na (229), Ca (225), Pb (225), Sr (225)
other solid-state systems	Kr (225), SiO_2 (152), SiO_2 (227), BN (216), AlN (216), AlN (186), SnO_2 (136), SnSe (62), SnTe (225), TiO_2 (136), TiO_2 (141), $SrTiO_3$ (221), MoS_2 (194), TiC (215), h-BN (194)

[a]The space group number is indicated in parentheses.

exchange−correlation energy density at a point in space depends only on properties (densities, density gradients, and kinetic energy densities) evaluated at that point. Global hybrid functionals, which replace a percentage of local exchange with nonlocal Hartree−Fock exchange,[40] are usually preferred for chemistry because they reduce delocalization error due to unphysical electron−electron self-interaction when one uses local functionals. However, including Hartree−Fock exchange globally make calculations too expensive for many applications to solids because Hartree−Fock exchange has high computer-time requirements in plane-wave codes. In addition, Hartree−Fock exchange leads to an anomalous divergence of the one-electron velocity at the Fermi level for metals.[41]

A major step forward for solid-state calculations by KS-DFT came in 2003, when Heyd, Scuseria, and Ernzerhof proposed a new density functional for calculating the exchange energy of a system based on the screened Coulomb potential called HSE03 (or HSE), which is a screened-exchange functional.[42] In such a functional, the percentage of Hartree−Fock exchange is not a global constant, as it depends on the interelectronic separation r and decreases to zero as r tends to ∞. This reduces the computational expense as compared to a global hybrid functional for plane-wave calculations on solids while maintaining the advantages of decreasing unphysical self-interaction.[43] Furthermore, the screening eliminates the spurious singularity for metals,[41] which allows one to introduce Hartree−Fock exchange to reduce self-interaction even for systems with no gap.

In 2006, Krukau et al.,[44] re-examined the impact of the exchange screening parameters and proposed a reparametrized version of HSE03, named HSE06, that replaces HSE03. Compared with the local functionals, the screened-exchange functional HSE06 is more accurate in terms of lattice constants and band gaps and is currently the preferred functional of most workers for band gap calculations.

Benchmark calculations are important in evaluating the performance of existing functionals and developing new functionals.[45−53] Tran and Blaha[49] constructed a database of 76 solid-state band gaps, including magnetic materials and solids with large band gaps, and used it to test band gap predictions using experimental lattice constants. They found the most accurate energy functionals (of those they tested, excluding a potential that does not have a corresponding energy functional) to be the global hybrid B3PW91 with a mean absolute error (MAE) of 0.73 eV, the surprisingly accurate local exchange functional AK13 with an MUE of 0.75 eV, and HSE06 with an MUE of 0.82 eV; however, they did not test the functionals mentioned in the next paragraph. Tang and Tao constructed a data set (22 data) of lattice constants for ionic solids consisting of alkali metal halides, silver halides, and other ionic solids.[54] Borlido et al. compiled a large data set (472 band gap data for nonmagnetic materials) to benchmark 12 functionals.[55] Their results again show good performance by HSE06. HSE06 performed well for these solid-state benchmarks, but few studies have evaluated the performance of other screened-exchange functionals.

Over the past decade, several additional screened-exchange functionals have been developed, such as N12-SX and MN12-SX proposed by Peverati and Truhlar in 2012[56] and HSE12 and HSE12s proposed by Moussa et al., also in 2012.[57] In 2020, we proposed M06-SX,[58] which added the screened HF exchange energy to our previously developed revM06-L[59] functional. The computational expense of any of these screened hybrid functionals is smaller than that of the global hybrid functionals, and here we test their relative accuracy for predicting band gaps and lattice constants of solid-state systems.

In this work, we focus on benchmarking the performance of screened-exchange functionals for electronic band gaps and lattice constants of solids. First, we compiled a lattice constant database called LC68 and a band gap database called BG60; these databases include Ge, BAs, GaAs, and InP, and other systems were added for the diversity of the data set. Second, we selected six screened-exchange functionals and six widely used or recently developed local functionals for the calculations. The performance of the selected functionals for band gaps and lattice constants is compared in detail.

2. METHODS AND COMPUTATIONAL DETAILS

2.1. Databases. The new databases (see Table 1) contain most of the solids considered in the literature[43,48,49,54,60,61] and include a large variety of solids, namely, metals, weakly bound solids, various semiconductors, ionic insulators, and transition-metal compounds.

The lattice constant database LC68 is a combination of four subdatabases: 31 common semiconductors (SLC31), 17 ionic insulators (ILC17), 5 metals (MLC5), and 15 other solids (OLC15). OLC15 includes strongly interacting crystals, ternary compounds, and oxide crystals.

Compared with LC68, the band gap database BG60 removes five metals and RbBr, TiC, and h-BN. The metals were removed because they have no band gap, and the three other compounds were removed because there are no experimental values for the band gaps. Thus, the BG60 database consists of three subdatabases: 31 common semiconductors (SBG31); 16 ionic insulators (IBG16), excluding RbBr; and 13 other solids (OBG13), excluding TiC and h-BN. The Cartesian coordinates, lattice constants, and band gaps that constitute the LC68 and BG60 databases are available in section S2 of the Supporting Information.

2.2. Basis Sets. To compute the LC68 and BG60 databases, the selection and modification methods of the basis sets and relativistic effective core potentials are obtained from ref 12. We used basis sets of Gaussian-type orbitals, and

https://doi.org/10.1021/acs.jctc.2c00822
J. Chem. Theory Comput. 2023, 19, 311−323

the basis sets used for different systems are listed in Table S1 (tables and figures with the prefix S are in the Supporting Information). For the elements of the first three periods, we started with the 6-311G* basis set. For heavier elements, except for Kr, we started with a small-core relativistic effective core potential with a polarized double-ζ valence basis set (cc-pVDZ-PP or Stuttgart-RSC-1997); for Kr, we started with the def2-TZVPP basis set. Modifications of these starting basis sets applied to solids are necessary for applications to solids because the highly optimized Gaussian basis sets developed in computational chemistry include low-exponent functions to simulate tails of wave functions, but these tails are not present in the interiors of solids.[12,48,62] These diffuse functions make the Coulomb near-field of the fast multipole method slower, unnecessarily slowing down the computation, and they lead to linear dependence in the basis set. Therefore, the starting basis sets in ref 12 were modified, primarily by deleting basis functions with exponents below 0.12, and we used these modified basis sets, which are denoted by an m-prefix, such as m-6-311G*, m-cc-pVDZ-PP, m-Stuttgart-RSC-1997. These modified basis sets are available in section S3 of the Supporting Information.

2.3. Functionals. Table 2 lists the names and types of all the functionals[22,32,34,44,56−59,63,64] used for computations in this work. There are six local functionals and six screened-exchange functionals. In terms of functional selection, we chose not only the popular functionals PBE, M06-L, and HSE06 but also newly developed functionals such as M06-SX, revM06-L, HLE17, and two interesting functionals developed in Chelikowsky's group, namely, HSE12 and HSE12s. Therefore, we not only focus on the difference between screened-exchange functionals and local functionals but also compare the performance of different screened-exchange functionals and assess the newly developed functionals.

Table 2. All the Functionals Computed in This Paper

name	type	ref
local functionals		
PBE	GGA	22
TPSS	meta-GGA	32
M06-L	meta-GGA	34
MN15-L	meta-NGA	63
revM06-L	meta-GGA	59
HLE17	meta-GGA	64
screened-exchange functionals		
HSE06	hybrid GGA	44
HSE12s	hybrid GGA	57
HSE12	hybrid GGA	57
MN12-SX	hybrid meta-NGA	56
N12-SX	hybrid NGA	56
M06-SX	hybrid meta-GGA	58

2.4. Calculations. We optimized the structures of the materials for every functional. We compare these equilibrium lattice constants directly to experiment, but the reader should keep in mind that experimental lattice constants represent—depending on the experiment—an average over the zero-point motion and possibly the thermal motion of the phonon vibrations. A previous study where this effect was estimated for 58 materials found an average increase in the calculated lattice constants of only 0.24% when the zero-point motion was included and also found little change in the error statistics of the calculated lattice constants.[61]

The band gaps were calculated with both the optimized lattice constants for that material and functional and the experimental geometry for each functional. The band gaps calculated here may be described as vertical band gaps in the sense of the Franck−Condon principle, which means that the lattice is frozen on the time scale of the electronic excitation.[65] Furthermore, as usual in this kind of calculation, we consider only the ground-state equilibrium structure and we do not average over the vibrational motion in the electronic ground state. If the excited state is long-lived and if the measurement yields the vibronic ground state rather than the vertical excitation energy, the band gap will also contain a contribution from the difference in the phonon zero-point energy between the excited state and the ground state. A straightforward way to account for the electron−phonon coupling upon the electronic excitation of the solid is to compute the phonon frequencies for the ground state occupation of the electronic bands and for the excited-state occupation.[66] At 0 K, all the phonon modes are in their ground state, and the resulting change in the zero-point energy would be added to the vertical electronic excitation energy; this correction is called zero-point renormalization (ZPR).[67] At nonzero temperatures, one can use thermal populations of the phonon modes to calculate the temperature dependence of the band gap. One can equivalently frame the problem as the effect of the phonon modes on the electronic energies.[66,67] Another contribution to the temperature dependence of the band gap is due to the expansion of the crystal as the temperature increases, usually decreasing the band gap; this effect is believed to be smaller than the change in phonon energy. Including full electron−phonon coupling considerably raises the effort;[68] it is usually not included, and is it not always clear whether it should be included for comparison to a particular experimental measurement. In the present work, we simply calculate the vertical gap without including electron−phonon coupling. The vertical gap (which is sometimes called the clamped-nuclei gap) is defined here as the lowest excitation energy at the fixed equilibrium lattice of the ground state. As an estimate of how large the neglected electron−phonon coupling effect on some measurements might be, we refer to two systematic studies. Karsai et al.[69] calculated the ZPRs of 18 semiconductors (all of which were 2−6, 3−5, or group 4 semiconductors); depending on the method, the median ZPR was only −0.06 or −0.05 eV. Engel et al.[68] studied 28 materials. For LiF, they calculated a ZPR of −1.23 eV; for 10 oxides, the average was −0.41 eV; and for the 17 other crystals (not a fluoride or oxide) in their study, the average was −0.12 eV. In all cases, the ZPR is negative, meaning that if one added it to the vertical excitation energy the predicted band gap would decrease.

The previous literature mainly emphasizes two motivations for developing screened-exchange functionals: cost considerations in plane-wave codes and the ability to eliminate the Hartree−Fock singularity at the Fermi level in metals even while gaining the advantages of Hartree−Fock exchange at small interelectronic distances. The latter motivation is important even in codes that do not use plane waves. Codes employing a linear combination of atom-centered basis functions (rather than or in addition to plane waves) for density functional calculations are also in wide use, and they are gaining more attention as they become more computationally efficient.[70−80] This makes the present study even more

https://doi.org/10.1021/acs.jctc.2c00822
J. Chem. Theory Comput. 2023, 19, 311−323

important, since hybrid functionals are relatively more affordable in codes employing linear combinations of atom-center basis functions. An example of a recent improvement in such a code is the recent extension by Dona et al. of the solid-state (sol-3c) DFT method in the CRYSTAL17 code, which improved the efficiency of the large-scale high-throughput screening of material properties.[78] Popular codes employing linear combinations of atom-centered basis functions include BAND,[72] which uses Slater-type basis functions, and CP2K,[76] CRYSTAL,[77] Gaussian,[81,82] PySCF,[74] and TURBOMOLE,[75] which use Gaussian-type basis functions. The present work uses Gaussian.

2.5. Software. All the calculations for the present work were carried out with Gaussian 09,[81] Gaussian 16,[82] and Minnesota Gaussian Functional Module (MN-GFM, ver. 6.11).[83] For calculations with periodic boundary conditions (PBC), we used the default *k*-point selection of the program for each system, ranging from 112 to 4044 *k*-points, with the most common number being 868. For each system, the *k*-points are the same for all functionals. The integration grid was set to (99, 590) to make the structural optimization robust.

2.6. Data Analysis. Experimental data were used as references to evaluate the performance of the functionals using performance statistics commonly used in benchmarking.[84] For each system and property x (calculated band gap value or lattice constant), there is a signed error err_x, which is the difference between the calculated value x_{cal} and experimental value x_{exp}.

$$\mathrm{err}_x = x_{\mathrm{cal}} - x_{\mathrm{exp}} \tag{1}$$

The mean signed error (MSE) is the arithmetic mean of the err_x

$$\mathrm{MSE} = \frac{1}{N}\sum_{x=1}^{N} \mathrm{err}_x \tag{2}$$

where N is 68 for LC68 and 60 for BG60. MSE underestimates the true error of the method due to the cancellation of errors with opposite signs;[85] therefore, we also consider the mean absolute error (MAE), also known as the mean unsigned error (MUE).[86]

$$\mathrm{MAE} = \mathrm{MUE} = \frac{1}{N}\sum_{x=1}^{N} |\mathrm{err}_x| \tag{3}$$

We use MAE as the primary statistic for evaluating functional performance. The root-mean-squared error (RMSE)[87] was calculated by

$$\mathrm{RMSE} = \sqrt{\frac{1}{N}\sum_{x=1}^{N} \mathrm{err}_x^{\,2}} \tag{4}$$

We also used the mean absolute percentage errors (MAPEs).

$$\mathrm{MAPE} = \frac{1}{N}\sum_{x=1}^{N} \left|\frac{\mathrm{err}_x}{x_{\mathrm{exp}}}\right| \tag{5}$$

The best-performing method should yield near-zero MSE values and low MAE, MAPE, and RMSE values.

3. RESULTS AND DISCUSSION

In this work, we collected 68 data for the lattice constant calculations and 60 data for the band gap calculations. All the systems are listed in Table 1, and the data and references are listed in Table S1. The data set is comprehensive and includes semiconductors (four representative systems, i.e., Ge, BAs, GaAs, and InP), ionic insulators, metals, oxides, weakly interacting crystals, ternary compounds, and oxide crystals. Six local and six screened-exchange hybrid functionals were chosen for comparison, as listed in Table 2.

3.1. Lattice Constants. We considered the lattice constants of 68 solid-state systems. Tables S2 and S3 show the results for the 68 lattice constants of six local functionals and six screened-exchange functionals. Table 3 presents the errors (Å) of these 12 functionals for the database LC68.

Table 3. Errors for the Lattice Constants Database (LC68) of 12 Functionals[a]

functional	MAE[b]	MSE[c]	RMSE[d]	MAPE[e]
screened-exchange				
M06-SX	0.051	0.011	0.089	0.96%
N12-SX	0.054	0.016	0.094	1.04%
HSE12s	0.068	0.035	0.118	1.26%
HSE12	0.068	0.038	0.123	1.26%
HSE06	0.074	0.047	0.127	1.38%
MN12-SX	0.085	0.041	0.192	1.55%
local				
M06-L	0.094	0.057	0.146	1.71%
revM06-L	0.099	0.058	0.240	1.78%
TPSS	0.102	0.074	0.179	1.90%
PBE	0.105	0.079	0.149	1.97%
MN15-L	0.107	0.047	0.159	1.96%
HLE17	0.122	−0.048	0.187	2.50%

[a]The functionals are sorted in ascending order of the MAEs. [b]MAE is the mean absolute error in Å, as shown in eq 3. [c]MSE is the mean signed error in Å, as shown in eq 2. [d]RMSE is the root-mean-squared error in Å, as shown in eq 4. [e]MAPE is the mean absolute percentage error, as shown in eq 5.

The MSE is a measure of systematic errors. Table 3 shows that 11 of the functionals have positive MSEs, ranging from 0.01 Å for M06-SX to 0.08 Å for PBE. We conclude that most density functionals tend to overestimate lattice constants.

Table 3 shows that we draw the same conclusions about the rank ordering of the top five functionals from MAE, RMSE, or MAPE. To streamline the discussion, we will focus it on MAEs, top performing functionals, and noteworthy special issues, but readers interested in more details of the statistics may consult the tables.

Table 3 shows that M06-SX and N12-SX give the smallest MAEs for LC68, with MAE values of 0.05 Å. M06-L and revM06-L have the lowest MAEs among the selected local functionals, with the values of 0.09−0.10 Å. The error statistics for MN12-SX and revM06-L are skewed by large errors for SnTe (absolute errors of 1.3 and 1.7 Å, respectively); eliminating SnTe decreases the MAEs to 0.022 and 0.033 Å, respectively.

The LC68 database can be divided into four subsets: 31 semiconductors (SLC31), 17 ionic insulators (ILC17), 5 metals (MLC5), and 15 other solid-state materials (OLC15). Tables S4−S7 list the error statistics for these subsets of the 12 selected functionals. Figure 1 shows the results of Tables S4−

https://doi.org/10.1021/acs.jctc.2c00822
J. Chem. Theory Comput. 2023, 19, 311−323

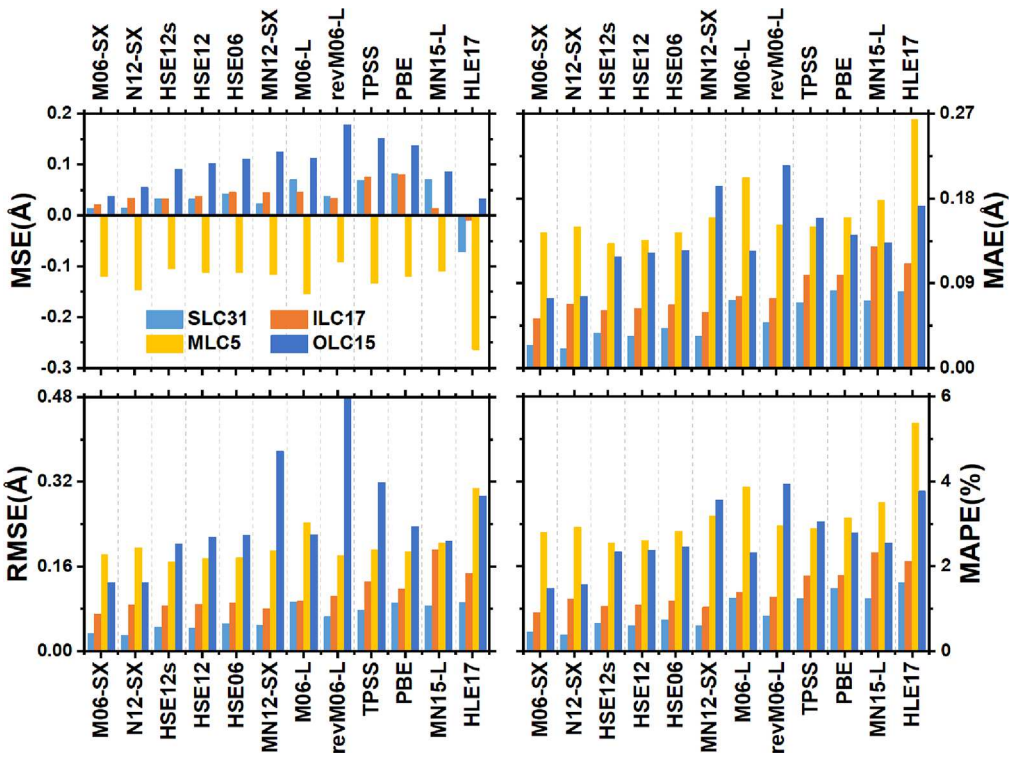

Figure 1. Results for the subdatabases of LC68 for 12 selected functionals. SLC31 contains the lattice constants of 31 common semiconductors, ILC17 contains the lattice constants of 17 ionic insulators, MLC5 contains the lattice constants of 5 metals, and OLC15 contains the lattice constants of 15 other solids (see Table 1).

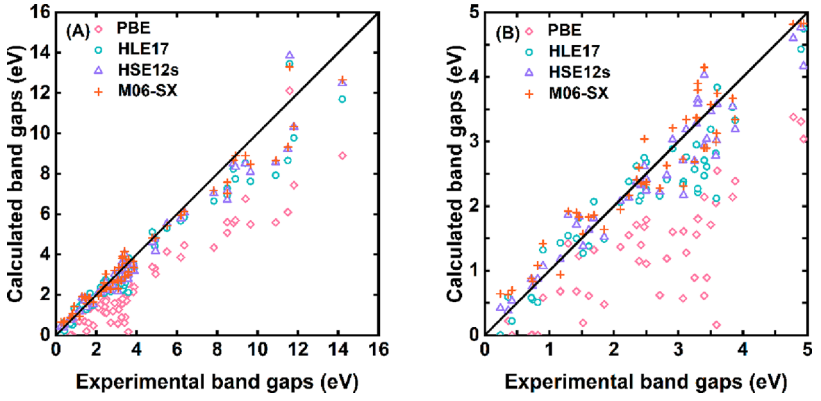

Figure 2. Calculated band gaps by PBE, HLE17, HSE12s, and M06-SX compared with the experimental values (eV).

S7 as bar graphs. The functionals are ordered in these tables and this figure in ascending order of the MAEs for LC68.

For SLC31, N12-SX and M06-SX give the best performance, with MAEs of 0.02 Å. If we considered only local functionals, we would recommend revM06-L for SLC31; the MAE is 0.05 Å. The MAE of HSE06, which is much more expensive than the local functionals, is 0.04 Å.

For ILC17, M06-SX and MN12-SX are the most accurate functionals, with MAEs of 0.05 and 0.06 Å, respectively. We find that revM06-L is the best local functional for ionic insulators, with a MAE of 0.07 Å.

For MLC5, the best functionals are HSE12s and HSE12, with MAEs of 0.13−0.14 Å. M06-SX and HSE06 are right behind with MAEs of 0.14 Å. The best local functionals are TPSS and revM06-L, with MAEs of 0.15 Å.

For OLC15, M06-SX and N12-SX give the smallest MAEs of 0.07−0.08 Å, with the third-best functional, HSE12s, some distance away at 0.12 Å. M06-L is the most accurate local functional, with a MAE again equal to 0.12 Å. However, revM06-L, which has the smallest MAEs for SLC31 and MLC5 and the second smallest MAE for ILC17 among the six local functionals, has the largest MAE among the 12 selected functionals; the main reason for the large mean errors of revM06-L and MN12-SX for OLC15 is, as already discussed, their poor performance for SnTe.

In summary, the best-performing functionals are N12-SX, M06-SX, HSE12s, and M06-SX for SLC31, ILC17, MLC5, and OLC15, respectively. These three functionals are also the best-performing functionals for the overall database LC68. Among the six local functionals, M06-L and revM06-L are the best performers for LC68 if we ignore SnTe.

3.2. Band Gaps at Consistently Optimized Geometries. The band gap database BG60 includes 60 of the 68 solid-state systems that were used for lattice constant

https://doi.org/10.1021/acs.jctc.2c00822
J. Chem. Theory Comput. 2023, 19, 311−323

calculations. In this section, we discuss band gaps calculated using the structure optimized by the functional under consideration. Tables S8 and S9 show the results for BG60 using the six local functionals and the six screened-exchange functionals.

By comparing the minimum gap to the minimum direct gap, it is possible to ascertain the type of gap, namely, direct or indirect. The results of Tables S8 and S9 refer to the minimum gap, which may be direct or indirect, and Tables S10 and S11 provide the minimum direct gap. Examination of the tables shows that the predicted band gap types of most materials are consistent among the functionals tested. The following solids have indirect band gaps with all functionals: Kr, C, Si, SiC, SiO_2, SiO_2, BN, BP, BAs, AlN, AlN, AlP, AlAs, AlSb, GaP, SnSe, SnTe, LiH, MgSe, CaF_2, BaS, BaSe, BaTe, TiO_2, $SrTiO_3$, MoS_2, AgCl, and AgBr; the space groups are given in Table 1.

Figure 2 shows the comparison of the calculated minimum band gaps and the experimental band gaps for PBE, HLE17, HSE12s, and M06-SX. The left plot of the figure shows all the calculated and experimental band gaps for BG60, and the right plot zooms in on band gaps lower than 5 eV. Figures S1−S12 show these kinds of plots for each functional. The diagonal lines in these figures indicate where the calculated band gap value would be equal to the experimental value.

As can be seen from these figures, the results of screened-exchange functionals are more accurate than the results of local functionals. The local functionals typically underestimate the band gaps, with most points to the right of the diagonals in the figures. PBE and TPSS underestimate the band gaps of almost all 60 systems in BG60. For the systems with large band gaps (higher than 5 eV), the screened-exchange functionals also show systematic underestimations. One exception is Kr, whose band gap is overestimated by most functionals. For the systems with small band gaps (lower than 2 eV), the local functionals underestimate the band gaps while the screened-exchange functionals overestimate them.

Table 4 shows the error statistics of the 12 selected functionals for BG60. As was the case for lattice constants, the screened-exchange functionals outperformed the local functionals for band gaps. The results are especially good for M06-SX, which gives the lowest MAE (0.47 eV) and RMSE (0.69 eV), although the MAPE of 17% is not the best. Another functional with a MAE lower than 0.5 eV is HSE12s (0.497 eV), which gives the lowest MAPE (12%) and the third lowest RMSE (0.78 eV). Among the local functionals, HLE17 is the best-performing functional, giving the lowest MAE (0.68 eV), RMSE (0.96 eV), and MAPE (19%); HLE17 is comparable in accuracy to the screened-exchange functional HSE06. The second-best-performing local functional is revM06-L.

Table 4. Errors for the Band Gaps of BG60 When Calculated with Consistently Optimized Lattice Constants[a]

functional	MAE[b]	MSE[c]	RMSE[d]	MAPE[e]
screened-exchange				
M06-SX	0.471	−0.165	0.689	17.3%
HSE12s	0.497	−0.296	0.775	12.0%
HSE12	0.527	−0.114	0.774	18.1%
N12-SX	0.578	−0.353	0.862	16.4%
MN12-SX	0.594	−0.383	0.890	15.9%
HSE06	0.679	−0.527	1.011	15.8%
local				
HLE17	0.677	−0.500	0.956	19.3%
revM06-L	0.875	−0.571	1.237	28.5%
MN15-L	1.266	−1.225	1.692	33.0%
M06-L	1.269	−1.219	1.626	35.3%
TPSS	1.595	−1.551	1.989	44.3%
PBE	1.770	−1.748	2.193	49.2%

[a]The functionals are sorted in ascending order of the MAEs. [b]MAE is the mean absolute error in eV, as shown in eq 3. [c]MSE is the mean signed error in eV, as shown in eq 2. [d]RMSE is the root-mean-squared error in eV, as shown in eq 4. [e]MAPE is the mean absolute percentage error, as shown in eq 5.

The MSEs of all functionals are negative, indicating that all functionals underestimate the band gaps on average. This is consistent with the results shown in Figures 2 and S1.

3.2.1. Subsets Organized by the Type of Solid. We divided BG60 into three subsets: SBG31, which includes 31 semiconductors; IBG16, with 16 ionic crystals; and OBG13, with 13 other solids. Tables S12−S15 list the error statistics of the 12 selected functionals for these subsets, which are sorted in the ascending order of the MAEs for BG60. Figure 3 shows the results of Tables S12−15 in bar graphs.

For SBG31, the smallest MAE is obtained by HSE12s (0.20 eV). N12-SX gives the smallest RMSE (0.30 eV) and the second-smallest MAE (0.24 eV). Among the local functionals, HLE17 is the best performer with the smallest MAE (0.31 eV). The revM06-L functional is the second-best local functional for SBG31, with an MAE of 0.45 eV.

The errors for ionic crystals are unacceptably large. M06-SX is the most accurate functional for IBG16, with the lowest MAE (0.85 eV), RMSE (1.09 eV), and MAPE (12%). We note that M06-SX is also the best of all the functionals for ILC17, so using M06-SX to calculate both the band gaps and the lattice constants of ionic insulators is recommended. The MAEs of HSE12s and HSE12 for IBG16 are 0.92 and 0.98 eV, making them second- and third-best. Among the local functionals, HLE17 has the smallest MAE, while its RMSE (1.50 eV) is smaller than those of MN12-SX (1.51 eV) and HSE06 (1.65 eV) and its MAPE (16%) is smaller than those of N12-SX (18%) and HSE06 (20%). Therefore, HLE17 is generally better than HSE06 and comparable to MN12-SX and N12-SX. In summary, M06-SX and HLE17 are the most-recommended screened-exchange and local functionals, respectively, for IBG16.

For OBG13, M06-SX gives the smallest MAE (0.55 eV), MN12-SX gives the smallest RMSE (0.69 eV), and HSE12s gives the smallest MAPE (14%). Among the local functionals, revM06-L and HLE17 are the best performers, with the lowest MAEs (0.86 and 0.90 eV, respectively), the lowest RMSEs (1.10 and 1.07 eV, respectively), and low MAPEs (26%). The lowest MAPE among local functionals is 24% from MN15-L.

Overall, M06-SX and HSE12s are the most-recommended functionals for band gap calculations. Among the local functionals, HLE17 gives the best results for SBG31 and IBG16 and the second-best result for OBG13, while revM06-L gives the second-best results for SBG31 and IBG16 and the best result for OBG31. Therefore, HLE17 and revM06-L are both recommended for band gap calculations among the local functionals.

3.2.2. Subsets Organized by the Size of the Band Gap. Because the band gaps of different systems vary greatly (spanning from 0 to 16 eV), we also divided BG60 into three subsets based on the experimental values of the band gaps, namely, "0−2 eV" (15 data), "2−5 eV" (30 data), and "5−16 eV" (15 data). Tables S16−S19 list the full error statistics of

https://doi.org/10.1021/acs.jctc.2c00822
J. Chem. Theory Comput. 2023, 19, 311−323

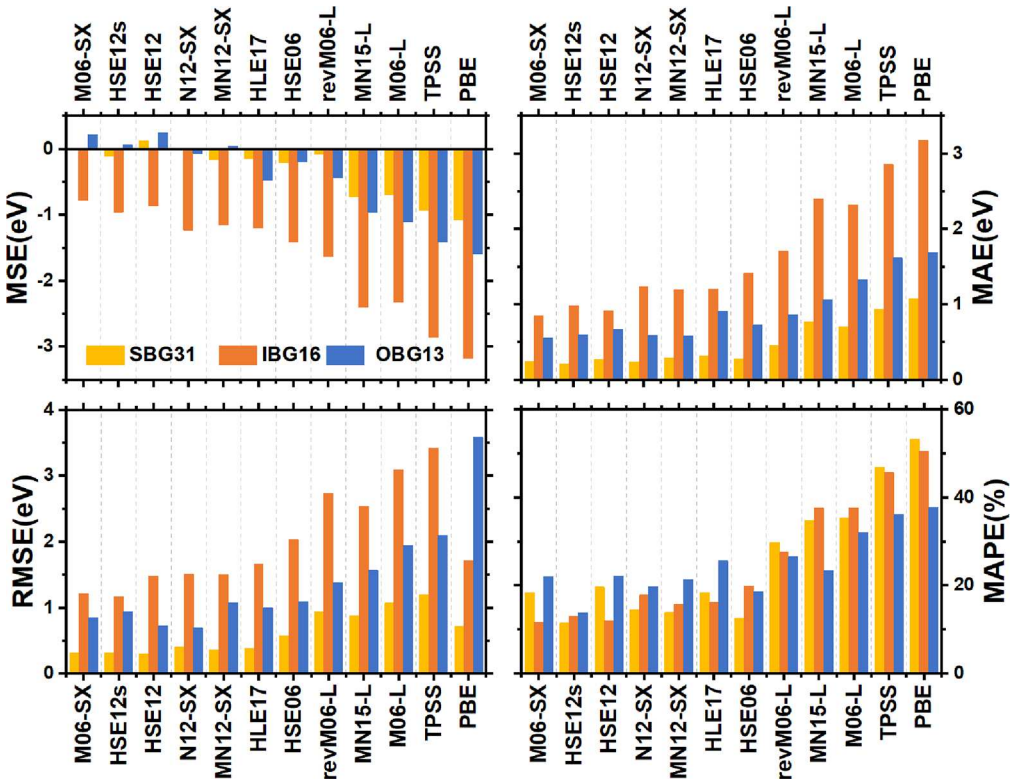

Figure 3. Results for the subdatabases of BG60 for 12 selected functionals. SBG31 contains 31 semiconductors, IBG16 contains 16 ionic insulators, and OBG13 contains 13 other solids (see Table S1).

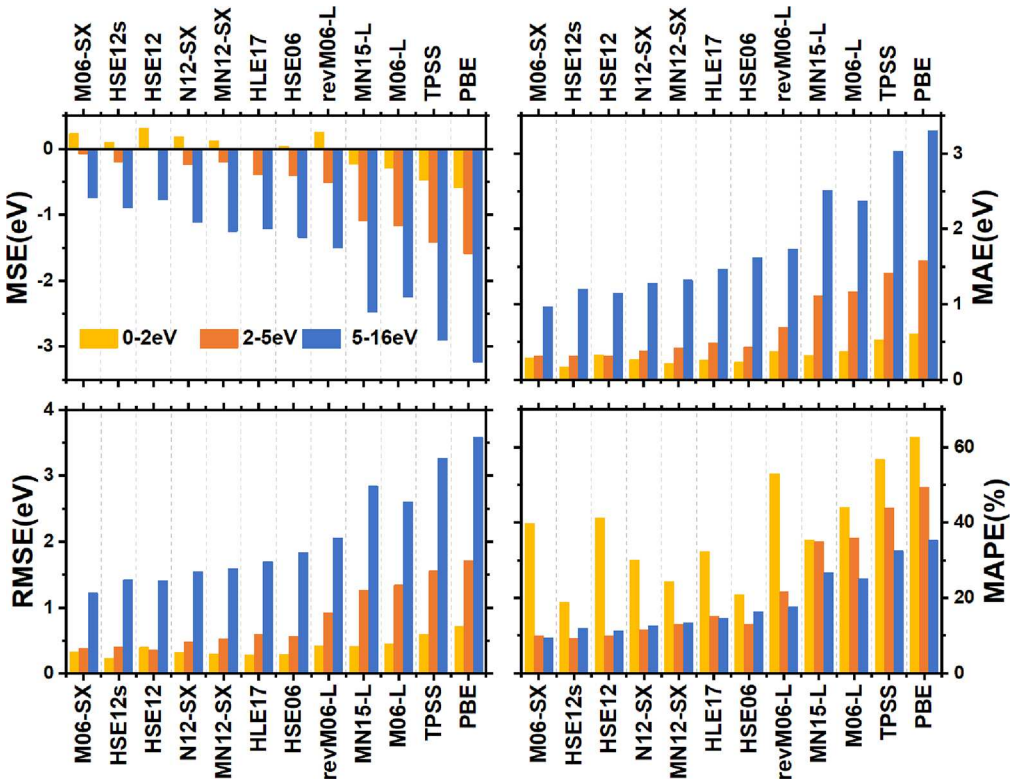

Figure 4. Results for the subdatabases of BG60 for 12 selected functionals. The BG60 is divided according to the experimental values of the band gaps, namely, "0−2 eV", "2−5 eV", and "5−16 eV".

the 12 selected functionals for these subsets, which are sorted in ascending order of the MAEs for BG60. Figure 4 shows the results of Tables S16−S19 in bar graphs.

For the "0−2 eV" subset, the smallest MAE (0.17 eV), RMSE (0.23 eV), and MAPE (19%) are obtained by the hybrid GGA functional HSE12. MN12-SX also performs well

https://doi.org/10.1021/acs.jctc.2c00822
J. Chem. Theory Comput. 2023, 19, 311−323

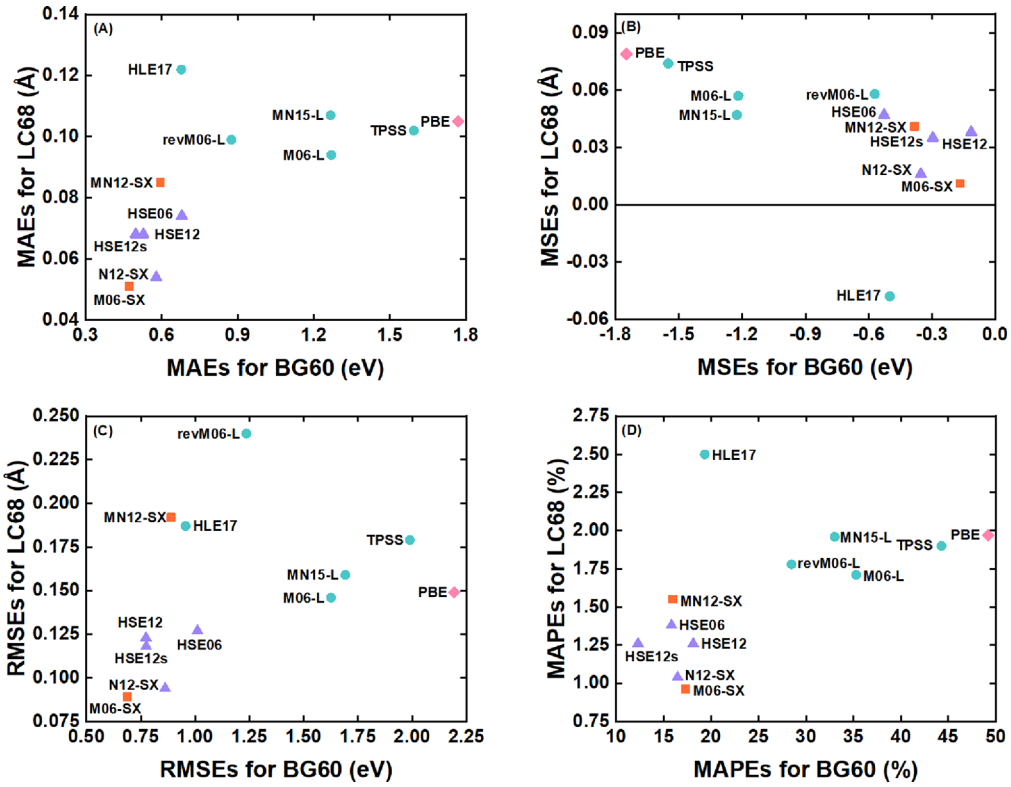

Figure 5. Statistical errors of each functional for BG60 and LC68.

for this subset, with a MAE of 0.22 eV. Among the local functionals, HLE17 and MN15-L perform the best, and their MAEs and MAPEs are lower than those of M06-SX and HSE12. HLE17 also gives a very low RMSE (0.275 eV), second only to HSE12s. The screened-exchange functionals tend to overestimate the band gaps of systems with small band gaps, and the local functionals tend to underestimate them. To sum up, the screened-exchange functional HSE12s and the local functional HLE17 are recommended for band gap calculations of systems with band gaps lower than 2 eV.

For the "2−5 eV" subset, HSE12s gives the smallest MAE (0.31 eV) and MAPE (9%) and a relatively small RMSE (0.40 eV). HSE12 and M06-SX also give good performances. The best local functional is HLE17, with MAE, RMSE, and MAPE of 0.49 eV, 0.59 eV, and 15%, respectively. Combined with the performance of the "0−2 eV" subset, the results show that the calculations of the systems with band gaps lower than 5 eV can be performed best by the screened-exchange functional HSE12s and the local functional HLE17.

For the "5−16 eV" subset, M06-SX is the most accurate among all the tested functionals, giving the lowest MAE (0.97 eV), RMSE (1.22 eV), and MAPE (10%). The MAEs of HSE12 and HSE12s are 1.15 and 1.20 eV, respectively, which are the second- and the third-smallest. The best local functional is HLE17, with MAE, RMSE, and MAPE of 1.47 eV, 1.70 eV, and 15%, respectively; these values are smaller than those of HSE06 (1.62 eV, 1.84 eV, and 16%). In summary, the hybrid meta-GGA M06-SX and meta-GGA HLE17 are recommended for the calculations of band gaps larger than 5 eV.

In summary, M06-SX and HSE12s are the most-recommended functionals for band gap calculations. HSE12s is more recommended for systems with small band gaps, and M06-SX is more recommended for systems with large band gaps. Among the local functionals, HLE17 gives the best results for all subsets. Therefore, HLE17 is recommended for band gap calculations among the local functionals.

By comparing Figures 1 and 3, we see that M06-SX gives the most balanced good performance for both lattice constants and band gaps of semiconductors and ionic crystals. HSE12s and N12-SX give relatively well-balanced results for other solids.

3.3. Band Gaps at Experimental Geometries. In this section, we discuss the band gap errors for each functional when the band gaps are based on the experimental lattice constants (LC-exp). Here and in the following section, the suffixes -opt and -exp are used to denote optimized and experimental structures, respectively. For each system in BG60, BG-opt and BG-exp are the band gaps calculated based on LC-opt and LC-exp, respectively. BG-opt and BG-exp were calculated with the same grid, convergence, and *k*-points to ensure that the results were comparable and only affected by the lattice constants. In Tables S20 and S21, we list the BG-exp values and statistical errors calculated by the local and screened-exchange functionals. Figure S13 shows the statistical errors (MAEs, MSEs, RMSEs, and MAPEs) of each functional for BG60-opt and BG60-exp. When a data point in this figure is near the diagonal, the band gaps are very similar for the two possible lattice constants; when a data point is close to the origin, the band gaps are most accurate. For the revM06-L, MN15-L, M06-L, and the screened-exchange functionals, the errors of BG60-opt and BG60-exp show little difference. The points for HLE17 in Figure S13 are located above the diagonal, and we see that HLE17 performs significantly better on BG60-opt than BG60-exp. For PBE and TPSS, the MAEs of BG60-exp are smaller than those of BG60-opt.

3.4. Overall Analysis. Figure 5 shows the statistical errors in band gaps and lattice constants for each functional, and different markers and colors are used for different types of

https://doi.org/10.1021/acs.jctc.2c00822
J. Chem. Theory Comput. 2023, 19, 311−323

functionals (squares represent hybrid meta-GAs, triangles represent hybrid GAs, circles represent meta-GAs, and the diamond represents the PBE GGA).

Figure 5A shows the MAEs of all the functionals for LC68 and BG60. As can be seen, all the screened-exchange functionals are in the lower-left portion of the figure, and the MAEs of screened-exchange functionals for both LC68 and BG60 are substantially smaller than those of the local functionals. M06-SX is positioned closet to the lower-left corner and is thus the best-performing functional. N12-SX is the second-best-performing functional for lattice constants and band gaps. Among the local functionals, revM06-L gives the second-best results for both LC68 and BG60.

Figure 5B shows the MSEs of the 12 selected functionals for the lattice constants and band gaps. It clearly shows that all the functionals have negative MSEs for BG60 and most functionals have positive MSEs for LC68. HLE17 is the only functional with a negative MSE for LC68.

Figure 5C shows the RMSE results; this figure mainly leads to the same conclusions as Figure 5A. The only significant exceptions are revM06-L and MN12-SX, where the RMSE is greatly increased by the bad prediction on SnTe.

Figure 5D shows the MAPEs. For LC68, the rankings sorted by the MAPEs are completely the same as those sorted by the MAEs. Moreover, the rankings for the subdatabases of LC68 sorted by the MAPEs are also almost the same as those sorted by the MAEs. However, for BG60, the rankings of the screened-exchange functionals sorted by the MAPEs are quite different from those sorted by the MAEs, and the MAPEs of other screened-exchange functionals are very close to each other except for HSE12s. The main reason for this difference is that the values of experimental band gaps vary widely. When calculating the percentage errors, a small error divided by a small experimental value (e.g., InSb 0.24 eV and SnTe 0.36 eV) would yield a large MAPE. Therefore, the influence of the small band gap systems is larger for MAPEs than for MAEs. As a result, HSE12s is recommended for band gap calculations of small band gap systems. The revM06-L functional gives the second smallest MAPEs for both LC68 and BG60.

HSE06 is known to provide useful accuracy for band gaps of solids with the efficiency of a screened-exchange functional, and it is widely used for that purpose; however, in the present analysis we find that there are recently developed screened-exchange density functionals that have superior performance compared to HSE06 for the calculation of solid-state properties. This illustrates that density functionals are still being improved.

HSE12 and HSE12s were developed by adjusting the overall fraction of Fock exchange and the length scale for exchange screening from HSE06.[57] Their functional forms are the same, but the results of HSE12 and HSE12s are clearly better than those of HSE06. We conclude that the parameter optimizations were very worthwhile. The M06-SX functional was developed based on revM06-L by adding a percentage of screened HF exchange energies. The M06-SX functional is clearly on the right track, improving the accuracy by nearly 47% on LC68 and reducing the MAE by 0.41 eV on BG60 as compared to revM06-L.

When developing revM06-L, MN15-L, M06-SX, MN12-SX, and N12-SX, the training set included LC18, which consists of 18 lattice-constant data (Li, Na, K, Al, NaCl, NaF, LiCl, LiF, MgO, Cu, Rh, Pd, Ag, Si, GaN (216), GaN (186), ZnSe, and InSb). Of these, 12 lattice constants (Li, Na, NaCl, NaF, LiCl, LiF, MgO, Si, GaN (216), GaN (186), ZnSe, and InSb) are included in LC68 of the present work. Table S22 lists the MAEs and rankings of the 12 tested functionals for LC18 and LC68. The results of LC18 are from refs 58 and 64. Table S22 shows that M06-SX and N12-SX show good transferability for lattice constants. However, the training on lattice constants is not always so effective. The MAE of revM06-L for LC18 is only 0.041 Å, which is only about half of that of M06-L, but the MAEs of revM06-L and M06-L for LC68 are similar to each other, with values of 0.099 and 0.094 Å, respectively. The optimization of the two parameters of HSE12 and HSE12s[57] involved the SC/40 database, which contains both band gaps and lattice constants of 40 solids. All 40 solids in SC/40 database are included in LC68 and BG60, and 5 of them are included in LC18. HSE12 and HSE12s show excellent performance for these databases. Therefore, parametrization does improve the performance of functionals for the trained properties, but the training set need to be large enough and diverse enough to ensure transferability.

3.5. Chemical Properties. For applications like catalysis, photocatalysis, and electrochemistry, we want functionals that not only give good solid-state properties but also give good chemistry. Tables S23 and S24 list the results of the 12 functionals studied here on the 26 subdatabases and 8 subdatabase groups of AME418 in Minnesota Database 2019; AME418 contains 418 atomic and molecular energetic data.[88] The results for HLE17 are calculated in this work, and the others are from reference 58. Tables S23 and S24 show that among the 12 functionals studied here, MN15-L, M06-SX, and revM06-L give the best performance for AME418, with MUEs of 2.29, 2.85, and 2.96 kcal/mol, respectively. For the chemical energies, the screened-exchange functionals do not always perform better than the local functionals, but M06-SX is a good compromise for applications involving heterogeneous chemistry studied with plane-wave codes. More generally, M06-SX and revM06-L are seen to give good performance for both solid-state chemistry and molecular chemistry and thus can be recommended for a wide range of applications.

4. CONCLUSIONS

In the present study, we constructed a lattice constant database LC68 and a band gap database BG60. We evaluated the performance of six screened-exchange functionals (HSE06, HSE12, HSE12s, MN12-SX, N12-SX, and M06-SX) and six local functionals (PBE, TPSS, M06-L, MN15-L, revM06-L, and HLE17) on both LC68 and BG60. We found that all screened-exchange functionals are superior to local functionals in terms of MAEs, RMSEs and MAPEs for these databases, and M06-SX is the best-performing functional for both BG60 and LC68 when evaluated by MAEs. The best local functionals for LC68 are M06-L and revM06-L, the best local functionals for BG60 are HLE17 and revM06-L, and the most well-balanced local functional among the six selected representative local functionals is revM06-L. Most functionals tend to overestimate the lattice constants and underestimate the band gaps.

We divided LC68 and BG60 into subsets and further analyzed which functionals are more suitable for specific kinds of systems. For lattice constants, N12-SX has the smallest MAE for simple binary semiconductors, M06-SX has outstanding performance for ionic insulators, and HSE12s is better than other functionals for metals. For band gap predictions, M06-SX is more suitable for ionic insulators and solids with large band gaps, and HSE12s performs better on semiconductors and

https://doi.org/10.1021/acs.jctc.2c00822
J. Chem. Theory Comput. 2023, 19, 311−323

solids with small band gaps. In conclusion, M06-SX performs better in general for both lattice constants and band gap predictions. The N12-SX and HSE12s functionals also show good performance for both band gaps and lattice constants. For local functionals, revM06-L and M06-L are the most highly recommended.

A final consideration is the performance of the various functionals for chemistry, since many applications, for example solar energy and heterogeneous photocatalysis, require not only good lattice constants and band gaps but also chemical thermodynamics and kinetics. M06-SX, revM06-L, and N12-SX not only have very good performance for the databases of this paper but also are well-optimized for chemical properties, as explained in previous papers[56,58,59] and shown in the Supporting Information.

■ ASSOCIATED CONTENT

Supporting Information

The Supporting Information is available free of charge at https://pubs.acs.org/doi/10.1021/acs.jctc.2c00822.

Basis sets, lattice constants, band gaps, and error statistics (PDF)

■ AUTHOR INFORMATION

Corresponding Authors

Ying Wang − *The National and Local Joint Engineering Laboratory of Animal Peptide Drug Development, College of Life Sciences, Hunan Normal University, Changsha, Hunan 410006, China;* orcid.org/0000-0002-4359-3753; Email: wangyin@hunnu.edu.cn

Donald G. Truhlar − *Department of Chemistry, Chemical Theory Center, University of Minnesota, Minneapolis, Minnesota 55455-0431, United States;* orcid.org/0000-0002-7742-7294; Email: truhlar@umn.edu

Zhonghua Liu − *The National and Local Joint Engineering Laboratory of Animal Peptide Drug Development, College of Life Sciences, Hunan Normal University, Changsha, Hunan 410006, China;* orcid.org/0000-0001-8497-6702; Email: liuzh@hunnu.edu.cn

Authors

Cheng Zhang − *The National and Local Joint Engineering Laboratory of Animal Peptide Drug Development, College of Life Sciences, Hunan Normal University, Changsha, Hunan 410006, China*

Pragya Verma − *Department of Chemistry, Chemical Theory Center, University of Minnesota, Minneapolis, Minnesota 55455-0431, United States;* orcid.org/0000-0002-5722-0894

Jiaxu Wang − *The National and Local Joint Engineering Laboratory of Animal Peptide Drug Development, College of Life Sciences, Hunan Normal University, Changsha, Hunan 410006, China*

Yiwei Liu − *Shanghai Engineering Research Center of Molecular Therapeutics and New Drug Development, Shanghai Frontiers Science Center of Molecule Intelligent Syntheses, School of Chemistry and Molecular Engineering, East China Normal University, Shanghai 200062, China*

Xiao He − *Shanghai Engineering Research Center of Molecular Therapeutics and New Drug Development, Shanghai Frontiers Science Center of Molecule Intelligent Syntheses, School of Chemistry and Molecular Engineering, East China Normal University, Shanghai 200062, China; New York University−East China Normal University Center for Computational Chemistry, New York University Shanghai, Shanghai 200062, China;* orcid.org/0000-0002-4199-8175

Complete contact information is available at: https://pubs.acs.org/10.1021/acs.jctc.2c00822

Author Contributions

The manuscript was written through contributions of all authors. Y.W., D.G.T., and Z.L. designed the research; C.Z., P.V., J.W., Y.L., X.H., Y.W., D.G.T., and Z.L. performed the research; C.Z., P.V., J.W., Y.L., X.H., Y.W., D.G.T., and Z.L. analyzed the data; and C.Z., P.V., J.W., Y.L., X.H., Y.W., D.G.T., and Z.L. wrote the paper. All authors have given approval to the final version of the manuscript.

Notes

The authors declare no competing financial interest.

■ ACKNOWLEDGMENTS

This work was supported in part by the National Natural Science Foundation of China (Grants 21903024, 32071262, and 31770832), the Natural Science Foundation of Hunan Province (Grant 2020JJ5349), and the Science and Technology Innovation Program of Hunan Province (Grant 2020RC4023). X.H. acknowledges the financial support from the National Natural Science Foundation of China (Grants 21922301 and 22273023), the National Key R&D Program of China (Grant 2019YFA0905200), the Shanghai Frontiers Science Center of Molecule Intelligent Syntheses, and the Fundamental Research Funds for the Central Universities. We thank the Bioinformatics Center of Hunan Normal University and the Supercomputer Center of East China Normal University (ECNU Multifunctional Platform for Innovation 001) for providing computer resources. The work at the University of Minnesota was supported in part by the National Science Foundation under Grant CHE-2054723.

■ REFERENCES

(1) Burke, K. Perspective on density functional theory. *J. Chem. Phys.* **2012**, *136* (15), 150901.

(2) Adekoya, D.; Qian, S.; Gu, X.; Wen, W.; Li, D.; Ma, J.; Zhang, S. DFT-Guided Design and Fabrication of Carbon-Nitride-Based Materials for Energy Storage Devices: A Review. *Nanomicro Lett.* **2021**, *13*, 13.

(3) Verma, P.; Truhlar, D. G. Status and Challenges of Density Functional Theory. *Trends in Chemistry* **2020**, *2* (4), 302−318.

(4) Yu, H. S.; Li, S. L.; Truhlar, D. G. Perspective: Kohn-Sham density functional theory descending a staircase. *J. Chem. Phys.* **2016**, *145* (13), 130901.

(5) Maurer, R. J.; Freysoldt, C.; Reilly, A. M.; Brandenburg, J. G.; Hofmann, O. T.; Björkman, T.; Lebègue, S.; Tkatchenko, A. Advances in Density-Functional Calculations for Materials Modeling. *Annu. Rev. Mater. Sci.* **2019**, *49* (1), 1−30.

(6) Patra, A.; Bates, J. E.; Sun, J.; Perdew, J. P. Properties of real metallic surfaces: Effects of density functional semilocality and van der Waals nonlocality. *Proc. Natl. Acad. Sci. U.S.A* **2017**, *114* (44), E9188−E9196.

(7) Anderson, L. N.; Aquino, F. W.; Raeber, A. E.; Chen, X.; Wong, B. M. Halogen Bonding Interactions: Revised Benchmarks and a New Assessment of Exchange vs Dispersion. *J. Chem. Theory Comput* **2018**, *14* (1), 180−190.

(8) He, Q.; Yu, B.; Li, Z.; Zhao, Y. Density Functional Theory for Battery Materials. *Energy & Environmental Materials* **2019**, *2* (4), 264−279.
(9) Liao, X.; Lu, R.; Xia, L.; Liu, Q.; Wang, H.; Zhao, K.; Wang, Z.; Zhao, Y. Density Functional Theory for Electrocatalysis. *Energy & Environmental Materials* **2022**, *5* (1), 157−185.
(10) Mancuso, J. L.; Mroz, A. M.; Le, K. N.; Hendon, C. H. Electronic Structure Modeling of Metal-Organic Frameworks. *Chem. Rev.* **2020**, *120* (16), 8641−8715.
(11) Brothers, E. N.; Izmaylov, A. F.; Normand, J. O.; Barone, V.; Scuseria, G. E. Accurate solid-state band gaps via screened hybrid electronic structure calculations. *J. Chem. Phys.* **2008**, *129* (1), 011102.
(12) Heyd, J.; Peralta, J. E.; Scuseria, G. E.; Martin, R. L. Energy band gaps and lattice parameters evaluated with the Heyd-Scuseria-Ernzerhof screened hybrid functional. *J. Chem. Phys.* **2005**, *123* (17), 174101.
(13) Schlüter, M.; Sham, L. J. Density-Functional Theory of the Band Gap. *Adv. Quantum Chem.* **1990**, *21*, 97−112.
(14) Lee, J.; Seko, A.; Shitara, K.; Nakayama, K.; Tanaka, I. Prediction model of band gap for inorganic compounds by combination of density functional theory calculations and machine learning techniques. *Phys. Rev. B Condens. Matter* **2016**, *93* (11), 115104.
(15) Li, Y.; Yang, W.; Dong, R.; Hu, J. Mlatticeabc: Generic Lattice Constant Prediction of Crystal Materials Using Machine Learning. *ACS Omega* **2021**, *6* (17), 11585−11594.
(16) Zhou, S.; Jin, K.; Buehler, M. J. Understanding Plant Biomass via Computational Modeling. *Adv. Mater.* **2021**, *33* (28), No. 2003206.
(17) Hohenberg, P.; Kohn, W. Inhomogeneous Electron Gas. *Phys. Rev.* **1964**, *136* (3B), B864−B871.
(18) Kohn, W.; Sham, L. J. Self-Consistent Equations Including Exchange and Correlation Effects. *Phys. Rev.* **1965**, *140* (4A), A1133−A1138.
(19) Perdew, J. P.; Yue, W. Accurate and simple density functional for the electronic exchange energy: Generalized gradient approximation. *Phys. Rev. B Condens. Matter* **1986**, *33* (12), 8800−8802.
(20) Becke, A. D. Density-functional exchange-energy approximation with correct asymptotic behavior. *Phys. Rev. A Gen. Phys.* **1988**, *38* (6), 3098−3100.
(21) Lee, C.; Yang, W.; Parr, R. G. Development of the Colle-Salvetti correlation-energy formula into a functional of the electron density. *Phys. Rev. B Condens. Matter* **1988**, *37* (2), 785−789.
(22) Perdew, J. P.; Burke, K.; Ernzerhof, M. Generalized gradient approximation made simple. *Phys. Rev. Lett.* **1996**, *77* (18), 3865−3868.
(23) Perdew, J. P.; Zunger, A. Self-interaction correction to density-functional approximations for many-electron systems. *Phys. Rev. B Condens. Matter* **1981**, *23* (10), 5048−5079.
(24) Haas, P.; Tran, F.; Blaha, P. Calculation of the lattice constant of solids with semilocal functionals. *Phys. Rev. B Condens. Matter* **2009**, *79* (8), 085104.
(25) Perdew, J. P.; Chevary, J. A.; Vosko, S. H.; Jackson, K. A.; Pederson, M. R.; Singh, D. J.; Fiolhais, C. Atoms, molecules, solids, and surfaces: Applications of the generalized gradient approximation for exchange and correlation. *Phys. Rev. B Condens. Matter* **1992**, *46* (11), 6671−6687.
(26) Becke, A. D. Density-functional thermochemistry. IV. A new dynamical correlation functional and implications for exact-exchange mixing. *J. Chem. Phys.* **1996**, *104* (3), 1040−1046.
(27) Armiento, R.; Mattsson, A. E. Functional designed to include surface effects in self-consistent density functional theory. *Phys. Rev. B Condens. Matter* **2005**, *72* (8), 085108.
(28) Becke, A. D.; Roussel, M. R. Exchange holes in inhomogeneous systems: A coordinate-space model. *Phys. Rev. A Gen. Phys.* **1989**, *39* (8), 3761−3767.
(29) Constantin, L. A.; Fabiano, E.; Della Sala, F. Meta-GGA Exchange-Correlation Functional with a Balanced Treatment of Nonlocality. *J. Chem. Theory Comput* **2013**, *9* (5), 2256−63.
(30) Perdew, J. P.; Ruzsinszky, A.; Csonka, G. I.; Constantin, L. A.; Sun, J. Workhorse semilocal density functional for condensed matter physics and quantum chemistry. *Phys. Rev. Lett.* **2009**, *103* (2), 026403.
(31) Sun, J.; Ruzsinszky, A.; Perdew, J. P. Strongly Constrained and Appropriately Normed Semilocal Density Functional. *Phys. Rev. Lett.* **2015**, *115* (3), 036402.
(32) Tao, J.; Perdew, J. P.; Staroverov, V. N.; Scuseria, G. E. Climbing the density functional ladder: Nonempirical meta-generalized gradient approximation designed for molecules and solids. *Phys. Rev. Lett.* **2003**, *91* (14), 146401.
(33) Van Voorhis, T.; Scuseria, G. E. A novel form for the exchange-correlation energy functional. *J. Chem. Phys.* **1998**, *109* (2), 400−410.
(34) Zhao, Y.; Truhlar, D. G. A new local density functional for main-group thermochemistry, transition metal bonding, thermochemical kinetics, and noncovalent interactions. *J. Chem. Phys.* **2006**, *125* (19), 194101.
(35) Zhao, Y.; Truhlar, D. G. Calculation of semiconductor band gaps with the M06-L density functional. *J. Chem. Phys.* **2009**, *130* (7), 074103.
(36) Perdew, J. P.; Tao, J.; Staroverov, V. N.; Scuseria, G. E. Meta-generalized gradient approximation: Explanation of a realistic nonempirical density functional. *J. Chem. Phys.* **2004**, *120* (15), 6898−911.
(37) Sun, J.; Marsman, M.; Ruzsinszky, A.; Kresse, G.; Perdew, J. P. Improved lattice constants, surface energies, and CO desorption energies from a semilocal density functional. *Phys. Rev. B Condens. Matter* **2011**, *83* (12), 121410.
(38) Sun, J.; Marsman, M.; Csonka, G. I.; Ruzsinszky, A.; Hao, P.; Kim, Y.-S.; Kresse, G.; Perdew, J. P. Self-consistent meta-generalized gradient approximation within the projector-augmented-wave method. *Phys. Rev. B Condens. Matter* **2011**, *84* (3), 035117.
(39) Tao, J.; Mo, Y. Accurate Semilocal Density Functional for Condensed-Matter Physics and Quantum Chemistry. *Phys. Rev. Lett.* **2016**, *117* (7), 073001.
(40) Becke, A. D. Density functional thermochemistry. III. The role of exact exchange. *J. Chem. Phys.* **1993**, *98*, 5648−5652.
(41) Ashcroft, N. W.; Mermin, N. D. *Solid State Physics*; Saunders College Publishing: Philadelphia, PA, 1976; pp 337 and 344.
(42) Heyd, J.; Scuseria, G. E.; Ernzerhof, M. Hybrid functionals based on a screened Coulomb potential. *J. Chem. Phys.* **2003**, *118* (18), 8207−8215.
(43) Peverati, R.; Truhlar, D. G. Quest for a universal density functional: The accuracy of density functionals across a broad spectrum of databases in chemistry and physics. *Philos. Trans A Math Phys. Eng. Sci.* **2014**, *372* (2011), 20120476.
(44) Krukau, A. V.; Vydrov, O. A.; Izmaylov, A. F.; Scuseria, G. E. Influence of the exchange screening parameter on the performance of screened hybrid functionals. *J. Chem. Phys.* **2006**, *125* (22), 224106.
(45) Womack, J. C.; Mardirossian, N.; Head-Gordon, M.; Skylaris, C. K. Self-consistent implementation of meta-GGA functionals for the ONETEP linear-scaling electronic structure package. *J. Chem. Phys.* **2016**, *145* (20), 204114.
(46) Mardirossian, N.; Head-Gordon, M. ωB97M-V: A combinatorially optimized, range-separated hybrid, meta-GGA density functional with VV10 nonlocal correlation. *J. Chem. Phys.* **2016**, *144* (21), 214110.
(47) Garza, A. J.; Bell, A. T.; Head-Gordon, M. Nonempirical Meta-Generalized Gradient Approximations for Modeling Chemisorption at Metal Surfaces. *J. Chem. Theory Comput* **2018**, *14* (6), 3083−3090.
(48) Peverati, R.; Truhlar, D. G. Performance of the M11-L density functional for bandgaps and lattice constants of unary and binary semiconductors. *J. Chem. Phys.* **2012**, *136* (13), 134704.
(49) Tran, F.; Blaha, P. Importance of the Kinetic Energy Density for Band Gap Calculations in Solids with Density Functional Theory. *J. Phys. Chem. A* **2017**, *121* (17), 3318−3325.

https://doi.org/10.1021/acs.jctc.2c00822
J. Chem. Theory Comput. 2023, 19, 311−323

(50) Tran, F.; Ehsan, S.; Blaha, P. Assessment of the GLLB-SC potential for solid-state properties and attempts for improvement. *Phys. Rev. Mater.* **2018**, *2* (2), 023802.
(51) Garza, A. J.; Scuseria, G. E. Predicting Band Gaps with Hybrid Density Functionals. *J. Phys. Chem. Lett.* **2016**, *7* (20), 4165−4170.
(52) Coskun, D.; Jerome, S. V.; Friesner, R. A. Evaluation of the Performance of the B3LYP, PBE0, and M06 DFT Functionals, and DBLOC-Corrected Versions, in the Calculation of Redox Potentials and Spin Splittings for Transition Metal Containing Systems. *J. Chem. Theory Comput* **2016**, *12* (3), 1121−8.
(53) Kim, S.; Lee, M.; Hong, C.; Yoon, Y.; An, H.; Lee, D.; Jeong, W.; Yoo, D.; Kang, Y.; Youn, Y.; Han, S. A band-gap database for semiconducting inorganic materials calculated with hybrid functional. *Sci. Data* **2020**, *7*, 387.
(54) Tang, H.; Tao, J. Comparative study of the properties of ionic solids from density functionals. *Mater. Res. Express* **2018**, *5* (7), 076302.
(55) Borlido, P.; Aull, T.; Huran, A. W.; Tran, F.; Marques, M. A. L.; Botti, S. Large-Scale Benchmark of Exchange-Correlation Functionals for the Determination of Electronic Band Gaps of Solids. *J. Chem. Theory Comput* **2019**, *15* (9), 5069−5079.
(56) Peverati, R.; Truhlar, D. G. Screened-exchange density functionals with broad accuracy for chemistry and solid-state physics. *Phys. Chem. Chem. Phys.* **2012**, *14* (47), 16187−91.
(57) Moussa, J. E.; Schultz, P. A.; Chelikowsky, J. R. Analysis of the Heyd-Scuseria-Ernzerhof density functional parameter space. *J. Chem. Phys.* **2012**, *136* (20), 204117.
(58) Wang, Y.; Verma, P.; Zhang, L.; Li, Y.; Liu, Z.; Truhlar, D. G.; He, X. M06-SX screened-exchange density functional for chemistry and solid-state physics. *Proc. Natl. Acad. Sci. U.S.A* **2020**, *117* (5), 2294−2301.
(59) Wang, Y.; Jin, X.; Yu, H. S.; Truhlar, D. G.; He, X. Revised M06-L functional for improved accuracy on chemical reaction barrier heights, noncovalent interactions, and solid-state physics. *Proc. Natl. Acad. Sci. U.S.A.* **2017**, *114* (32), 8487−8492.
(60) Tran, F.; Stelzl, J.; Blaha, P. Rungs 1 to 4 of DFT Jacob's ladder: Extensive test on the lattice constant, bulk modulus, and cohesive energy of solids. *J. Chem. Phys.* **2016**, *144* (20), 204120.
(61) Hao, P.; Fang, Y.; Sun, J.; Csonka, G. I.; Philipsen, P. H. T.; Perdew, J. P. Lattice constants from semilocal density functionals with zero-point phonon correction. *Phys. Rev. B Condens. Matter* **2012**, *85* (1), 014111.
(62) Crowley, J. M.; Tahir-Kheli, J.; Goddard, W. A., 3rd Resolution of the Band Gap Prediction Problem for Materials Design. *J. Phys. Chem. Lett.* **2016**, *7* (7), 1198−203.
(63) Yu, H. S.; He, X.; Truhlar, D. G. MN15-L: A New Local Exchange-Correlation Functional for Kohn-Sham Density Functional Theory with Broad Accuracy for Atoms, Molecules, and Solids. *J. Chem. Theory Comput* **2016**, *12* (3), 1280−93.
(64) Verma, P.; Truhlar, D. G. HLE17: An Improved Local Exchange−Correlation Functional for Computing Semiconductor Band Gaps and Molecular Excitation Energies. *J. Phys. Chem. C* **2017**, *121* (13), 7144−7154.
(65) Marder, M. P. *Condensed Matter Physics*, 1st ed.; Wiley: New York, NY, 2000; p 628−629.
(66) King-Smith, R. D.; Needs, R. J.; Heine, V.; Hodgson, M. J. A First-Principle Calculation of the Temperature Dependence of the Indirect Band Gap of Silicon. *Europhys. Lett.* **1989**, *10*, 569−574.
(67) Poncé, S.; Antonius, G.; Gillet, Y.; Boulanger, P.; Janssen, J. L.; Marini, A.; Côté, M.; Gonze, X. Temperature dependence of electronic eigenenergies in the adiabatic harmonic approximation. *Phys. Rev. B* **2014**, *90*, 214304.
(68) Engel, M.; Miranda, H.; Chaput, L.; Togo, A.; Verdi, C.; Marsman, M.; Kresse, G. Zero-point Renormalization of the Band Gap of Semiconductors and Insulators Using the PAW Method. *Phys. Rev. B* **2022**, *106* (9), 094316.
(69) Karsai, F.; Engel, M.; Flage-Larsen, E.; Kresse, G. Electron−phonon coupling in semiconductors within the GW approximation. *New J. Phys.* **2018**, *20* (12), 123008.
(70) Callahan, J. M.; Lange, M. F.; Berkelbach, T. C. Dynamical correlation energy of metals in large basis sets from downfolding and composite approaches. *J. Chem. Phys.* **2021**, *154* (21), 211105.
(71) te Velde, G.; Baerends, E. J. Precise density-functional method for periodic structures. *Phys. Rev. B Condens Matter* **1991**, *44* (15), 7888−7903.
(72) Verzijl, C. J. O.; Thijssen, J. M. DFT-Based Molecular Transport Implementation in ADF/BAND. *J. Phys. Chem. C* **2012**, *116* (46), 24393−24412.
(73) Bulik, I. W.; Scalmani, G.; Frisch, M. J.; Scuseria, G. E. Noncollinear Density Functional Theory Having Proper Invariance and Local Torque Properties. *Phys. Rev. B* **2013**, *87*, 035117.
(74) Sun, Q.; Zhang, X.; Banerjee, S.; Bao, P.; Barbry, M.; Blunt, N. S.; Bogdanov, N. A.; Booth, G. H.; Chen, J.; Cui, Z. H.; Eriksen, J. J.; Gao, Y.; Guo, S.; Hermann, J.; Hermes, M. R.; Koh, K.; Koval, P.; Lehtola, S.; Li, Z.; Liu, J.; Mardirossian, N.; McClain, J. D.; Motta, M.; Mussard, B.; Pham, H. Q.; Pulkin, A.; Purwanto, W.; Robinson, P. J.; Ronca, E.; Sayfutyarova, E. R.; Scheurer, M.; Schurkus, H. F.; Smith, J. E. T.; Sun, C.; Sun, S. N.; Upadhyay, S.; Wagner, L. K.; Wang, X.; White, A.; Whitfield, J. D.; Williamson, M. J.; Wouters, S.; Yang, J.; Yu, J. M.; Zhu, T.; Berkelbach, T. C.; Sharma, S.; Sokolov, A. Y.; Chan, G. K. Recent developments in the PySCF program package. *J. Chem. Phys.* **2020**, *153* (2), 024109.
(75) Balasubramani, S. G.; Chen, G. P.; Coriani, S.; Diedenhofen, M.; Frank, M. S.; Franzke, Y. J.; Furche, F.; Grotjahn, R.; Harding, M. E.; Hättig, C.; Hellweg, A.; Helmich-Paris, B.; Holzer, C.; Huniar, U.; Kaupp, M.; Marefat Khah, A.; Karbalaei Khani, S.; Müller, T.; Mack, F.; Nguyen, B. D.; Parker, S. M.; Perlt, E.; Rappoport, D.; Reiter, K.; Roy, S.; Rückert, M.; Schmitz, G.; Sierka, M.; Tapavicza, E.; Tew, D. P.; van Wüllen, C.; Voora, V. K.; Weigend, F.; Wodyński, A.; Yu, J. M. TURBOMOLE: Modular program suite for ab initio quantum-chemical and condensed-matter simulations. *J. Chem. Phys.* **2020**, *152*, 184107.
(76) Kühne, T. D.; Iannuzzi, M.; Del Ben, M.; Rybkin, V. V.; Seewald, P.; Stein, F.; Laino, T.; Khaliullin, R. Z.; Schütt, O.; Schiffmann, F.; et al. CP2K: An electronic structure and molecular dynamics software Package − Quickstep: Efficient and accurate electronic structure calculations. *J. Chem. Phys.* **2020**, *152*, 194103.
(77) Dovesi, R.; Pascale, F.; Civalleri, B.; Doll, K.; Harrison, N. M.; Bush, I.; D'Arco, P.; Noel, Y.; Rerat, M.; Carbonniere, P.; Causa, M.; Salustro, S.; Lacivita, V.; Kirtman, B.; Ferrari, A. M.; Gentile, F. S.; Baima, J.; Ferrero, M.; Demichelis, R.; De La Pierre, M. The CRYSTAL code, 1976−2020 and beyond, a long story. *J. Chem. Phys.* **2020**, *152* (20), 204111.
(78) Dona, L.; Brandenburg, J. G.; Bush, I. J.; Civalleri, B. Cost-effective composite methods for large-scale solid-state calculations. *Faraday Discuss.* **2020**, *224* (0), 292−308.
(79) Lee, J.; Feng, X.; Cunha, L. A.; Gonthier, J. F.; Epifanovsky, E.; Head-Gordon, M. Approaching the basis set limit in Gaussian-orbital-based periodic calculations with transferability: Performance of pure density functionals for simple semiconductors. *J. Chem. Phys.* **2021**, *155* (16), 164102.
(80) Sharma, S.; Beylkin, G. Efficient Evaluation of Two-Center Gaussian Integrals in Periodic Systems. *J. Chem. Theory Comput* **2021**, *17* (7), 3916−3922.
(81) Frisch, M. J.; Trucks, G. W.; Schlegel, H. B.; Scuseria, G. E.; Robb, M. A.; Cheeseman, J. R.; Scalmani, G.; Barone, V.; Petersson, G. A.; Nakatsuji, H.; Li, X.; Caricato, M.; Marenich, A. V.; Bloino, J.; Janesko, B. G.; Gomperts, R.; Mennucci, B.; Hratchian, H. P.; Ortiz, J. V.; Izmaylov, A. F.; Sonnenberg, J. L.; Williams; Ding, F.; Lipparini, F.; Egidi, F.; Goings, J.; Peng, B.; Petrone, A.; Henderson, T.; Ranasinghe, D.; Zakrzewski, V. G.; Gao, J.; Rega, N.; Zheng, G.; Liang, W.; Hada, M.; Ehara, M.; Toyota, K.; Fukuda, R.; Hasegawa, J.; Ishida, M.; Nakajima, T.; Honda, Y.; Kitao, O.; Nakai, H.; Vreven, T.; Throssell, K.; Montgomery, J. A., Jr.; Peralta, J. E.; Ogliaro, F.; Bearpark, M. J.; Heyd, J. J.; Brothers, E. N.; Kudin, K. N.; Staroverov, V. N.; Keith, T. A.; Kobayashi, R.; Normand, J.; Raghavachari, K.; Rendell, A. P.; Burant, J. C.; Iyengar, S. S.; Tomasi, J.; Cossi, M.; Millam, J. M.; Klene, M.; Adamo, C.; Cammi, R.; Ochterski, J. W.;

https://doi.org/10.1021/acs.jctc.2c00822
J. Chem. Theory Comput. 2023, 19, 311−323

Martin, R. L.; Morokuma, K.; Farkas, O.; Foresman, J. B.; Fox, D. J. *Gaussian 09*, rev. C.01; Gaussian, Inc.: Wallingford, CT, 2010.
(82) Frisch, M. J.; Trucks, G. W.; Schlegel, H. B.; Scuseria, G. E.; Robb, M. A.; Cheeseman, J. R.; Scalmani, G.; Barone, V.; Petersson, G. A.; Nakatsuji, H.; Li, X.; Caricato, M.; Marenich, A. V.; Bloino, J.; Janesko, B. G.; Gomperts, R.; Mennucci, B.; Hratchian, H. P.; Ortiz, J. V.; Izmaylov, A. F.; Sonnenberg, J. L.; Williams; Ding, F.; Lipparini, F.; Egidi, F.; Goings, J.; Peng, B.; Petrone, A.; Henderson, T.; Ranasinghe, D.; Zakrzewski, V. G.; Gao, J.; Rega, N.; Zheng, G.; Liang, W.; Hada, M.; Ehara, M.; Toyota, K.; Fukuda, R.; Hasegawa, J.; Ishida, M.; Nakajima, T.; Honda, Y.; Kitao, O.; Nakai, H.; Vreven, T.; Throssell, K.; Montgomery, J. A., Jr.; Peralta, J. E.; Ogliaro, F.; Bearpark, M. J.; Heyd, J. J.; Brothers, E. N.; Kudin, K. N.; Staroverov, V. N.; Keith, T. A.; Kobayashi, R.; Normand, J.; Raghavachari, K.; Rendell, A. P.; Burant, J. C.; Iyengar, S. S.; Tomasi, J.; Cossi, M.; Millam, J. M.; Klene, M.; Adamo, C.; Cammi, R.; Ochterski, J. W.; Martin, R. L.; Morokuma, K.; Farkas, O.; Foresman, J. B.; Fox, D. J. *Gaussian 16*, rev. C.01; Gaussian, Inc.: Wallingford, CT, 2016.
(83) Zhao, Y.; Peverati, R.; Yang, K.; Luo, S.; Yu, H.; He, X.; Wang, Y.; Verma, P.; Truhlar, D. G. *MN-GFM*, ver. 6.11; University of Minnesota: Minneapolis, MN, **2019**.
(84) Olejniczak, A.; Cichy, B.; Stręk, W. DFT calculations of metal-organic I-III-VI semiconductor clusters: Benchmark of exchange-correlation functionals and localized basis sets. *Comput. Mater. Sci.* **2019**, *163*, 186−195.
(85) Pernot, P.; Civalleri, B.; Presti, D.; Savin, A. Prediction Uncertainty of Density Functional Approximations for Properties of Crystals with Cubic Symmetry. *J. Phys. Chem. A* **2015**, *119* (21), 5288−5304.
(86) Ruscic, B. Uncertainty quantification in thermochemistry, benchmarking electronic structure computations, and Active Thermochemical Tables. *Int. J. Quantum Chem.* **2014**, *114* (17), 1097−1101.
(87) Chai, T.; Draxler, R. R. Root mean square error (RMSE) or mean absolute error (MAE)? − Arguments against avoiding RMSE in the literature. *Geosci. Model Dev* **2014**, *7* (3), 1247−1250.
(88) Wang, Y.; Verma, P.; Jin, X.; Truhlar, D. G.; He, X. Revised M06 density functional for main-group and transition-metal chemistry. *Proc. Natl. Acad. Sci. U. S. A* **2018**, *115* (41), 10257−10262.

https://doi.org/10.1021/acs.jctc.2c00822
J. Chem. Theory Comput. 2023, 19, 311−323